

Pulsed electrodeposition of $(\text{Bi}_{1-x}\text{Sb}_x)_2\text{Te}_3$ thermoelectric thin films

DORIANE DEL FRARI, SEBASTIEN DILIBERTO*, NICOLAS STEIN, CLOTILDE BOULANGER and JEAN-MARIE LECUIRE

Laboratoire d'Electrochimie des Materiaux, UMR 7555, Universite Paul Verlaine, Metz, 1 Bd Arago, Technopôle, CP 87811, F-57078, Metz Cedex 3, France

(*author for correspondence, fax: +33-3-8731-5460, e-mail: sebastien.diliberto@univ-metz.fr)

Received 6 June 2005; accepted in revised form 1 November 2005

Key words: bismuth antimony telluride, electrodeposition, pulsed technique, thermoelectric properties, thin films

Abstract

$(\text{Bi}_{1-x}\text{Sb}_x)_2\text{Te}_3$ thermoelectric thin films were deposited on stainless steel discs in 1 M perchloric acid and 0.1 M tartaric acid by pulse electrodeposition in order to optimize the grain growth. The influence of the electrolyte composition, the cathodic current density and the cathodic pulse time on film stoichiometry were studied. The results show that it is necessary to increase the Sb content in the electrolyte to obtain the $(\text{Bi}_{0.25}\text{Sb}_{0.75})_2\text{Te}_3$ film stoichiometry. Pulse plating reduced the grain size and the roughness, compared with continuous plating. Thermoelectric and electrical properties were also studied and it was found that the Seebeck coefficient and electrical resistivity were related to two parameters: the cathodic pulse current density and the films thickness.

1. Introduction

Considerable interest has developed in alternative refrigeration and cooling technologies. Thermoelectric cooling devices based upon the Peltier effect have been used for many years in many applications such as thermoelectric generators [1, 2], coolers [3] and for optical storage systems [4]. Bismuth telluride represents the parent compound of a family of technologically important semiconductor alloys that are used extensively in modern thermoelectric coolers [5, 6]. These alloys possess a high figure of merit ZT due to a high Seebeck coefficient (α), moderate electrical conductivity (σ) and low thermal conductivity (λ). In addition, increased use of thermoelectric coolers for temperature stabilisation of electronic components has led to miniaturisation of thermoelectric coolers. The current tendency to miniaturisation has provoked interest in thin film thermoelectric devices. The electrochemical process is a particularly attractive route for processing thin film semiconductor materials [7]. It offers the advantages of a low synthesis temperature, a simple and low cost preparation of thin or thick samples and a large area deposition on a laboratory scale.

Electrodeposition has been successfully applied to the production of bismuth telluride binaries [8–12] and Bi–Te–Se ternaries [13] in 1 M nitric acid, for potentiostatic and galvanostatic ways. Recently, the optimum conditions for potentiostatic plating of Bi–Sb–Te were determined [14]. An electrolyte (HClO_4 1 M and $\text{C}_4\text{H}_6\text{O}_6$ 0.1 M) was used to electrodeposit the ternary. By varying the electrode potential and the electrolyte composition, it

was possible to achieve a large range of ternary film compositions, in particular $(\text{Bi}_{0.25}\text{Sb}_{0.75})_2\text{Te}_3$ which presents the best thermoelectric properties at room temperature [15]. However, $(\text{Bi}_{1-x}\text{Sb}_x)_2\text{Te}_3$ films obtained by steady state methods present significant roughness.

In order to optimize the material morphology synthesis by pulsed current electrodeposition was studied. This technique is an advanced form of electrodeposition which offers better control over deposit properties by controlling the interfacial electrochemical reaction. A number of variables such as pulse waveform, cathodic/anodic pulses, ON/OFF pulse time or duty cycle, applied and mean current density, etc., offers effective ways to control macroscopic properties such as better adhesion, crack free hard deposits, fine grained films with uniformity and lower porosity [16–20]. The present work concerns, in particular, the definition of the optimum conditions for a pulse electrodeposition of $(\text{Bi}_{1-x}\text{Sb}_x)_2\text{Te}_3$, through a comparison of the different pulse parameter influences. The morphology of these films was analysed in order to obtain a higher rate of grain nucleation and a more refined grain structure. Finally, pulsed parameters and the thickness dependence of electrical and thermoelectric properties of Bi–Sb–Te films were studied.

2. Experimental details

2.1. Deposition conditions

Pulsed electrodeposition refers to deposition where a current density is rapidly alternated between two

different values. In the simplest case, this is realized with a series of pulses of equal amplitude, duration and polarity. Each pulse consists of an "ON" time T_{on} during which a cathodic current density J_c is applied, and an "OFF" time T_{off} during which zero current density $J_a = 0 \text{ A dm}^{-2}$ is applied (Figure 1). The average current density J_m is defined as $J_m = J_c \{T_{\text{on}} / (T_{\text{on}} + T_{\text{off}})\}$.

Stainless steel discs were chosen as substrate for the pulsed deposition experiments. Plates were mechanically polished with silicon paper followed by diamond paste ($1 \mu\text{m}$ size). After being polished, the electrodes were cleaned with distilled water followed by rinsing with ethanol. The working electrodes were located horizontally in the bottom of a polytetrafluoroethylene (PTFE) cell which had an electrolyte volume of 0.1 dm^3 , under an argon atmosphere. A 2 cm^2 area was exposed for deposition, which was carried out at room temperature without stirring. The electrochemical potentials of the working electrode were measured and expressed by reference to a saturated calomel electrode (SCE) and the counter electrode was a platinum disc (1 cm^2). The experiments were realized using a Radiometer PGZ 301 potentiostat, Voltmaster 4 software. The electrolytic baths were prepared with Millipore™ water ($10 \text{ m } \Omega\text{m}$) and analytical grade reagents. To ensure the stability and the solubility of bismuth(III), antimony(III) and tellurium(IV) species in solution, the selected solvent was a solution containing tartaric acid (0.1 M) chosen for its chelating properties in relation to antimony, and perchloric acid (1 M) for its acid properties. The solutions were respectively obtained by dissolution of Bi_2O_3 , Sb_2O_3 and TeO_2 . According to previous work using the continuous method [14], the cation ratio $([\text{Bi}] + [\text{Sb}]) / [\text{Te}]$ was fixed at 1, and the value of the $[\text{Sb}] / [\text{Bi}]$ ratio varied from 3 to 8. The tellurite concentration was fixed at 10^{-2} M for all the mixtures. Except for the study of the thickness influence, all films were deposited with a thickness of $5 \mu\text{m}$, which corresponds to a total deposition time of 4100 s according to Faraday's law.

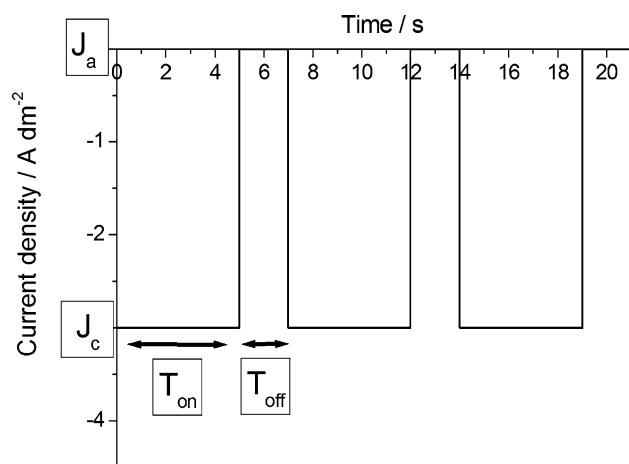


Fig. 1. Theoretical diagram of the pulse plating electrodeposition process.

2.2. Deposition characterizations

Samples were prepared after electrodeposition by thorough rinsing in three steps (nitric acid solution pH 1, Millipore™ water and ethanol) followed by drying in air. X-ray diffraction data were obtained with an Inel diffractometer (XRG 2500 CPS 120, CoK_α or CuK_α radiation). The sample composition was obtained by electron probe microanalysis (CAMECA SX 50 and SX 100). Ten different measures were performed and the stoichiometry was assessed using the average of these 10 values. Analysis was reproducible within $\pm 1\%$. The morphology was studied using a scanning electron microscope SEM (HITACHI model S 2500 LB) and the roughness was measured with a vertical scanning interferometer (Wyko® NT1100 Optical Profiler).

The electrical properties of the electrodeposited $(\text{Bi}_{1-x}\text{Sb}_x)_2\text{Te}_3$ materials were determined by measuring the Seebeck coefficient and electrical resistivity. The Seebeck coefficient was measured at room temperature using a Keithley 2700 multimeter. The temperatures and the differential potential of the film were measured using 0.1 mm diameter K type standard thermocouples. The voltage was measured between two probes held at a fixed distance of 2 cm from each other. The hot probe was heated to a temperature of $2 \text{ }^\circ\text{C}$ above the other one. Electrical resistivity was measured using the four point technique, with an HEM-2000 EGK system at a constant current of $1 \times 10^{-3} \text{ A}$. All annealings of $200 \text{ }^\circ\text{C}$ were realized in a Thermolyne 21100 tube furnace under primary vacuum.

3. Results and discussion

According to previous work [14] a tartaric-perchloric electrolyte with a $([\text{Bi}] + [\text{Sb}]) / [\text{Te}]$ cation ratio equal to 1, a $[\text{Sb}] / [\text{Bi}]$ ratio equal to 3 and $[\text{Te}] = 10^{-2} \text{ M}$, allows $(\text{Bi}_{1-x}\text{Sb}_x)_2\text{Te}_3$ electroplating with a potentiostatic method. In particular, the $(\text{Bi}_{0.25}\text{Sb}_{0.75})_2\text{Te}_3$ ternary, which is considered to have the best thermoelectric properties at room temperature, is obtained for a large potential range from -0.15 to -0.25 V vs. SCE. The surface feature of a sample with this stoichiometry, obtained for a deposition potential of -0.17 V vs. SCE, was examined by SEM. A representative micrograph is shown in Figure 2. The film has significant roughness due to heterogeneous grain growth. Indeed, the deposit has a crystallized arborescent form in which 5 to $30 \mu\text{m}$ grain clusters were measured. A measurement by interferometric microscopy gave a root mean square (RMS) roughness of $8.61 \mu\text{m}$.

In order to optimize the material morphology synthesis by pulsed current electrodeposition was studied.

3.1. Influence of pulsed deposition parameters

The pulsed deposition process allows control of the cation concentration at the cathode/solution interface

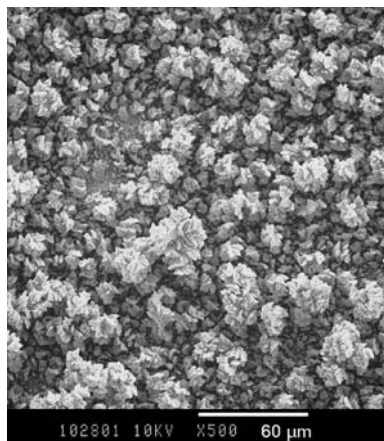


Fig. 2. SE micrograph of a $(\text{Bi}_{0.25}\text{Sb}_{0.75})_2\text{Te}_3$ electrodeposited film – $E_{\text{deposition}} = -0.17$ V vs. SCE, $[\text{Bi}^{\text{III}+}] + [\text{Sb}^{\text{III}+}] = [\text{Te}^{\text{IV}+}] = 10^{-2}$ M, $[\text{Sb}^{\text{III}+}]/[\text{Bi}^{\text{III}+}] = 3$, Thickness = $5 \mu\text{m}$.

by independently changing the pulse parameters, such as cathodic current density J_c , cathodic pulse duration T_{on} and time between pulses T_{off} .

Initially, the electrolyte giving the $(\text{Bi}_{0.25}\text{Sb}_{0.75})_2\text{Te}_3$ ternary, that is $([\text{Bi}] + [\text{Sb}])/[\text{Te}] = 1$ and $[\text{Sb}]/[\text{Bi}] = 3$, was chosen and the influence of cathodic current density J_c and on-time T_{on} were studied. Previous voltammetric studies allow T_{off} to be fixed at 10 s to ensure that the interfacial species concentrations at the electrode returned to their initial values. Figure 3 shows the cathodic current density dependence of the film composition for an on-time of 3 s. The dotted lines represent the expected stoichiometry. For all the range studied the curves show that the bismuth and tellurium contents increase with decreasing cathodic current density, in contrast to the antimony content which decreases strongly. In addition, the morphology evolves from a

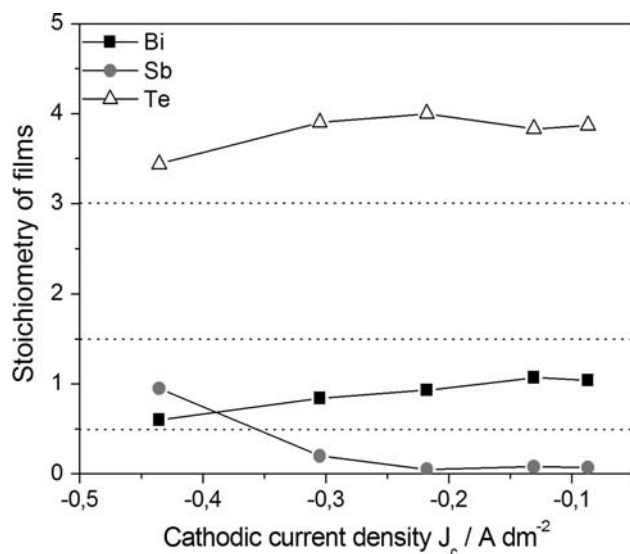


Fig. 3. Cathodic intensity dependence of $\text{Bi}_x\text{Sb}_y\text{Te}_z$ stoichiometry – $[\text{Bi}^{\text{III}+}] + [\text{Sb}^{\text{III}+}] = [\text{Te}^{\text{IV}+}] = 10^{-2}$ M, $[\text{Sb}^{\text{III}+}]/[\text{Bi}^{\text{III}+}] = 3$ – $T_{\text{on}} = 3$ s, $T_{\text{off}} = 10$ s, $J_a = 0$ A dm^{-2} , Thickness = $5 \mu\text{m}$.

powdery to a metallic aspect when the cathodic current density decreases. From a less cathodic current density than -1.3×10^{-1} A dm^{-2} , the film peels off the substrate during synthesis. This phenomenon is probably due to strong internal stress resulting from hydrogen generation on the electrode.

In order to investigate the influence of the on-time on the stoichiometry the cathodic current density was fixed at -2.15×10^{-1} A dm^{-2} . This value represents a current density for which the film does not peel off and is not powdery. The results are presented in Figure 4. It was observed that bismuth and tellurium stoichiometries decrease with increasing cathodic pulse time, in contrast with the antimony content which increases strongly.

For deposition times lower than 3 s the films contain little antimony and they peel off during synthesis. When T_{on} is more than 7 s, the stoichiometry is close to $(\text{Bi}_{0.25}\text{Sb}_{0.75})_2\text{Te}_3$, but the films have a powdery morphology which is equivalent to that obtained with the continuous method [14]. For an on-time of 5 s, the electrodeposit has a much less disturbed morphology than in the case of continuous synthesis (Figure 5). The roughness measurement of $2.24 \mu\text{m}$ confirms this result. On the other hand, the Sb content in the film is not sufficient. Pulse current synthesis allows optimization of the film morphology by choosing a high cathodic current density J_c or a short on-time. But, it seems that the roughness improvement is accompanied by a decrease in the Sb content in the film. This phenomenon was already observed by Fleurial et al. [11].

In order to get closer to $(\text{Bi}_{0.25}\text{Sb}_{0.75})_2\text{Te}_3$, the $[\text{Sb}]$ concentration in the solution was increased. Two ratios were chosen: $[\text{Sb}]/[\text{Bi}] = 6$ and $[\text{Sb}]/[\text{Bi}] = 8$, whereas the $([\text{Bi}] + [\text{Sb}])/[\text{Te}]$ ratio was kept at 1. As before, J_c was fixed at -2.15×10^{-1} A dm^{-2} ; the evolution of the stoichiometry of films vs. the on-time is represented on Figures 6 and 7 for the two ratios. The other parameters

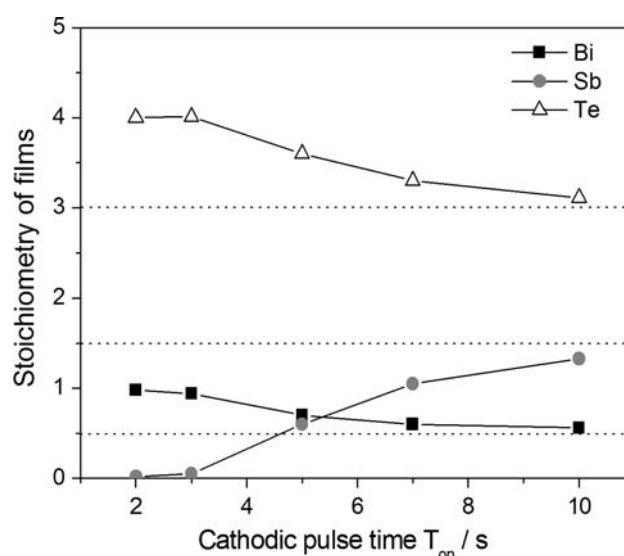


Fig. 4. Cathodic pulse time dependence of $\text{Bi}_x\text{Sb}_y\text{Te}_z$ stoichiometry – $[\text{Bi}^{\text{III}+}] + [\text{Sb}^{\text{III}+}] = [\text{Te}^{\text{IV}+}] = 10^{-2}$ M, $[\text{Sb}^{\text{III}+}]/[\text{Bi}^{\text{III}+}] = 3$ – $T_{\text{off}} = 10$ s, $J_c = -2.15 \times 10^{-1}$ A dm^{-2} , $J_a = 0$ A dm^{-2} , Thickness = $5 \mu\text{m}$.

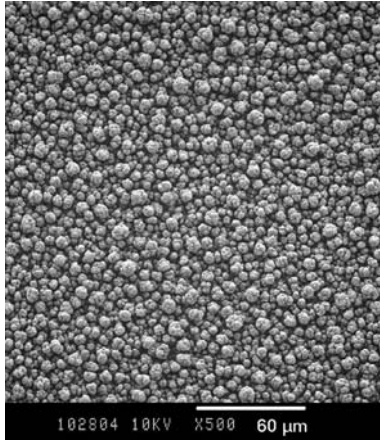


Fig. 5. SE micrograph of a $(\text{Bi}_{0.54}\text{Sb}_{0.46})_{1.4}\text{Te}_{3.60}$ electrodeposited film – $[\text{Bi}^{\text{III}}] + [\text{Sb}^{\text{III}}] = [\text{Te}^{\text{IV}}] = 10^{-2}$ M, $[\text{Sb}^{\text{III}}]/[\text{Bi}^{\text{III}}] = 3$ – $T_{\text{on}} = 5$ s, $T_{\text{off}} = 10$ s, $J_c = -2.15 \times 10^{-1}$ A dm^{-2} , $J_a = 0$ A dm^{-2} , Thickness = 5 μm .

were fixed at $T_{\text{off}} = 5$ s and $J_a = 0$ A dm^{-2} . In each case two distinct areas can be observed. For short deposition times film stoichiometries present a high Te content and a very low Sb one. When T_{on} increases the Te content rapidly decreases until it reaches a value of 3 and the Bi content slowly decreases, while the Sb stoichiometry increases. This is especially observed in the case of $[\text{Sb}]/[\text{Bi}] = 8$. When the on-time was more than 4 s the stoichiometry was close to $(\text{Bi}_{0.25}\text{Sb}_{0.75})_2\text{Te}_3$ and remained almost constant whatever the on-time.

The films present a different morphology, in spite of their similar stoichiometries. The SEM observation confirmed the same evolution as previously. When T_{on} increased the electrodeposits became increasingly powdery. Figure 8 shows a micrograph of the film obtained at $T_{\text{on}} = 5$ s, $[\text{Sb}]/[\text{Bi}] = 8$ with a $(\text{Bi}_{0.17}\text{Sb}_{0.83})_2\text{Te}_{2.99}$ stoichiometry. The film is constituted of small 3 μm

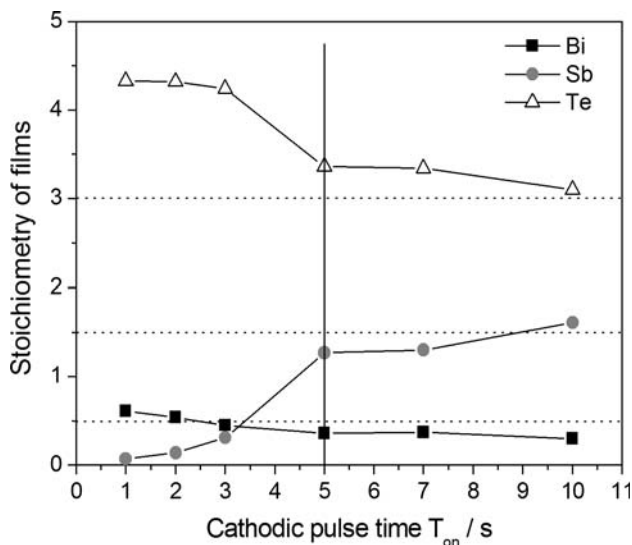


Fig. 6. Cathodic pulse time dependence of $\text{Bi}_x\text{Sb}_y\text{Te}_z$ stoichiometry – $[\text{Bi}^{\text{III}}] + [\text{Sb}^{\text{III}}] = [\text{Te}^{\text{IV}}] = 10^{-2}$ M, $[\text{Sb}^{\text{III}}]/[\text{Bi}^{\text{III}}] = 6$ – $T_{\text{off}} = 5$ s, $J_c = -2.15 \times 10^{-1}$ A dm^{-2} , $J_a = 0$ A dm^{-2} , Thickness = 5 μm .

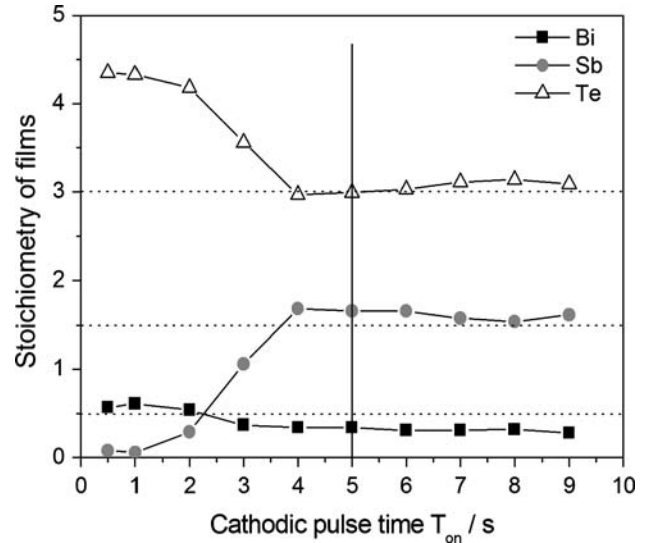


Fig. 7. Cathodic pulse time dependence of $\text{Bi}_x\text{Sb}_y\text{Te}_z$ stoichiometry – $[\text{Bi}^{\text{III}}] + [\text{Sb}^{\text{III}}] = [\text{Te}^{\text{IV}}] = 10^{-2}$ M, $[\text{Sb}^{\text{III}}]/[\text{Bi}^{\text{III}}] = 8$ – $T_{\text{off}} = 5$ s, $J_c = -2.15 \times 10^{-1}$ A dm^{-2} , $J_a = 0$ A dm^{-2} , Thickness = 5 μm .

diameter spherical grains. However, Figure 9 presents the electrodeposit surface obtained with a 9 s on-time. The surface is strongly disturbed and presents the same non-homogeneous growth and unpredictable arborescent form as observed in continuous electrodeposition. The evolution of the morphology is illustrated in Figure 10 with the RMS measurements. The value of the RMS decreases strongly from 10 to 1 μm as the cathodic pulse time decreases. This reduction in grain size, already observed [18], can be explained by the reduction of on-time with a consequent increase in the number of new grains nucleated, producing a more compact deposit and a more refined grain structure.

However, a too strong decrease of the on-time leads to modification of the stoichiometry and the morphology optimization is associated with a significant decrease in the Sb stoichiometry in the film.

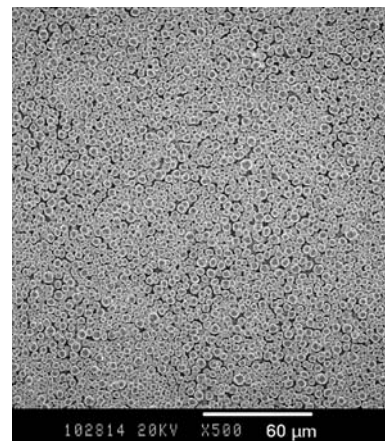


Fig. 8. SE micrograph of a $(\text{Bi}_{0.17}\text{Sb}_{0.83})_2\text{Te}_{2.99}$ electrodeposited film – $[\text{Bi}^{\text{III}}] + [\text{Sb}^{\text{III}}] = [\text{Te}^{\text{IV}}] = 10^{-2}$ M, $[\text{Sb}^{\text{III}}]/[\text{Bi}^{\text{III}}] = 8$ – $T_{\text{on}} = 5$ s, $T_{\text{off}} = 5$ s, $J_c = -2.15 \times 10^{-1}$ A dm^{-2} , $J_a = 0$ A dm^{-2} , Thickness = 5 μm .

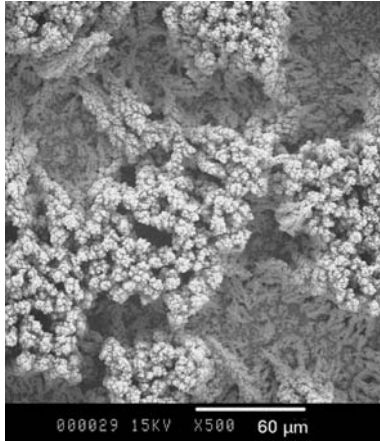


Fig. 9. SE micrograph of a $(\text{Bi}_{0.15}\text{Sb}_{0.85})_{1.90}\text{Te}_{3.09}$ electrodeposited film – $[\text{Bi}^{\text{III}+}] + [\text{Sb}^{\text{III}+}] = [\text{Te}^{\text{IV}+}] = 10^{-2}$ M, $[\text{Sb}^{\text{III}+}]/[\text{Bi}^{\text{III}+}] = 8$ – $T_{\text{on}} = 9$ s, $T_{\text{off}} = 5$ s, $J_c = -2.15 \times 10^{-1}$ A dm^{-2} , $J_a = 0$ A dm^{-2} , Thickness = $5 \mu\text{m}$.

3.2. Thermoelectric properties

Thermoelectric properties were studied for films obtained by pulse plating in order to assess the influence of the pulse parameters. The Seebeck coefficient α and the electrical resistivity ρ were measured, so the power factor α^2/ρ could be determined. The optimal cation ratios and pulse parameters defined previously were chosen to study the on-time dependence of the thermoelectric properties.

All samples present a p-type behaviour immediately after synthesis, which is consistent with the literature [15]. Before the measurement of Seebeck coefficient and electrical resistivity, all films were annealed at 200°C for 1 h under argon. Indeed, it was proved that thermoelectric properties are improved with annealing [21], without modifying the film composition. Figure 11

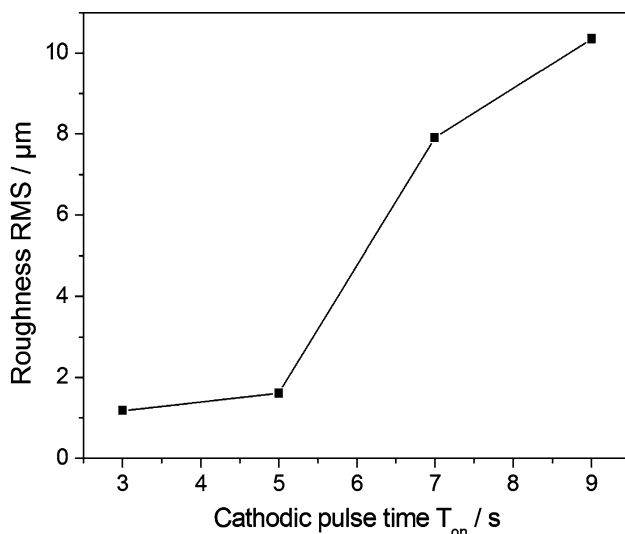


Fig. 10. Cathodic pulse time dependence of roughness – $[\text{Bi}^{\text{III}+}] + [\text{Sb}^{\text{III}+}] = [\text{Te}^{\text{IV}+}] = 10^{-2}$ M, $[\text{Sb}^{\text{III}+}]/[\text{Bi}^{\text{III}+}] = 8$ – $T_{\text{off}} = 5$ s, $J_c = -2.15 \times 10^{-1}$ A dm^{-2} , $J_a = 0$ A dm^{-2} , Thickness = $5 \mu\text{m}$.

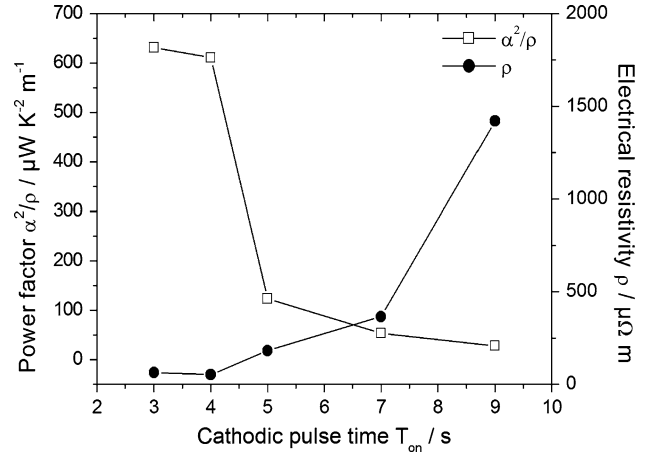


Fig. 11. Evolution of power factor and electrical resistivity with cathodic pulse time – $[\text{Bi}^{\text{III}+}] + [\text{Sb}^{\text{III}+}] = [\text{Te}^{\text{IV}+}] = 10^{-2}$ M, $[\text{Sb}^{\text{III}+}]/[\text{Bi}^{\text{III}+}] = 8$ – $T_{\text{off}} = 5$ s, $J_c = -2.15 \times 10^{-1}$ A dm^{-2} , $J_a = 0$ A dm^{-2} , Thickness = $5 \mu\text{m}$.

shows the variation of the power factor α^2/ρ vs. the on-time. Two areas can be defined and are similar to those observed for the stoichiometry. In the first one ranging between 3 and 5 s, pulse plating films have a high power factor of about $600 \mu\text{W K}^{-2} \text{m}^{-1}$. At an on-time of 5 s, the power factor decreases to $100 \mu\text{W K}^{-2} \text{m}^{-1}$ and evolves to $50 \mu\text{W K}^{-2} \text{m}^{-1}$ as the on-time increases. In fact, the very small value of α^2/ρ is directly related to the evolution of ρ , whereas the Seebeck coefficient remained constant at $180 \mu\text{V K}^{-1}$. This value can be compared with the $40\text{--}300 \mu\text{V K}^{-1}$ range measured by Fleurial et al. [11] for $(\text{Bi}_{0.25}\text{Sb}_{0.75})_2\text{Te}_3$ electrodeposited films. However, other techniques such as flash evaporation [22] or MOCVD [23] allows a Seebeck coefficient value of $240 \mu\text{V K}^{-1}$ to be obtained for the same film composition. The evolution of ρ must be correlated with the roughness of the films (Figure 10). The figure shows that a high on-time leads to a film with a high degree of roughness and such a morphology implies a very high

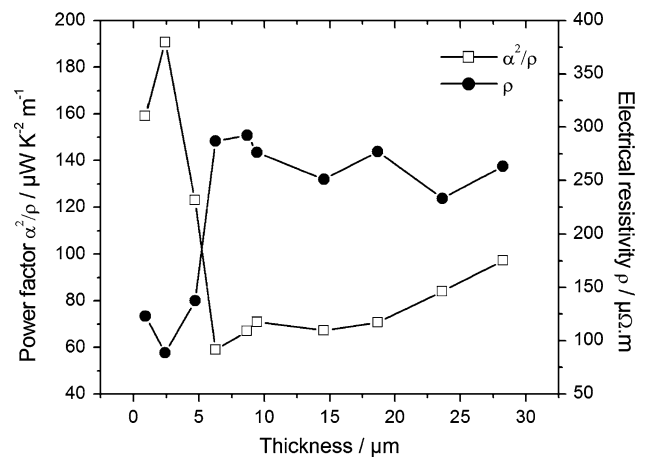


Fig. 12. Evolution of power factor and electrical resistivity with film thickness – $[\text{Bi}^{\text{III}+}] + [\text{Sb}^{\text{III}+}] = [\text{Te}^{\text{IV}+}] = 10^{-2}$ M, $[\text{Sb}^{\text{III}+}]/[\text{Bi}^{\text{III}+}] = 8$ – $T_{\text{on}} = 5$ s, $T_{\text{off}} = 5$ s, $J_c = -2.15 \times 10^{-1}$ A dm^{-2} , $J_a = 0$ A dm^{-2} .

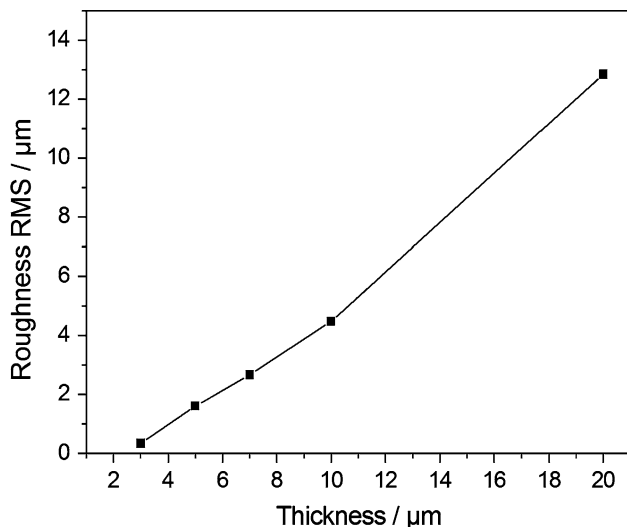


Fig. 13. Thickness dependence of roughness – $[\text{Bi}^{\text{III}+}] + [\text{Sb}^{\text{III}+}] = [\text{Te}^{\text{IV}+}] = 10^{-2}$ M, $[\text{Sb}^{\text{III}+}]/[\text{Bi}^{\text{III}+}] = 8$ – $T_{\text{on}} = 5$ s, $T_{\text{off}} = 5$ s, $J_c = -2.15 \times 10^{-1}$ A dm^{-2} , $J_a = 0$ A dm^{-2} .

electrical resistivity. Consequently, in this case the evolution of the power factor is directly dependent on the roughness of the film and its influence on the electrical resistivity.

The same conclusion can be made concerning the evolution of the power factor with the thickness of the film (Figure 12). Several electrodepositions were conducted with the following parameters: $J_c = -2.15 \times 10^{-1}$ A dm^{-2} , $T_{\text{on}} = 5$ s, $T_{\text{off}} = 5$ s, $J_a = 0$ A dm^{-2} , for appropriate numbers of cycles to obtain different thicknesses. Each film presents the same $(\text{Bi}_{0.25}\text{Sb}_{0.75})_2\text{Te}_3$ stoichiometry whatever the thickness. These alloys crystallize with rhombohedral structure (R-3 m) and the grain size, which was calculated with the Scherrer equation, is between 500 and 600 Å whatever the film thicknesses. Figure 13 shows a linear evolution of roughness with thickness, which leads to a strong decrease in the power factor when the thickness is over 5 μm . For smaller thicknesses ($e \leq 5$ μm), films have excellent electrical resistivity which is inferior to 150 $\mu\Omega$ m, and consequently a power factor around 190 $\mu\text{W K}^{-2} \text{m}^{-1}$.

4. Conclusion

An electrolyte (HClO_4 1 M and $\text{C}_4\text{H}_6\text{O}_6$ 0.1 M) has been used to electrodeposit Bi–Sb–Te ternaries by pulse plating. Study of the different parameters has established their influence on the film stoichiometry. The grain size decreases with decrease in on-time and a high compactness is achieved. Pulsed electrodeposition allows deposits with a substantial thickness of 10 μm to be obtained showing better thermoelectric and electrical properties than films obtained in continuous plating, with a power factor which increases from 52 [21] to

100 $\mu\text{W K}^{-2} \text{m}^{-1}$. The best synthesis parameters are a $[\text{Sb}]/[\text{Bi}]$ ratio of 8, a cathodic current density J_c of -2.15×10^{-1} A dm^{-2} and an on-time value of 5 s, equal to the off-time.

Acknowledgements

The authors are indebted to the Service Commun de Microanalyse (UHP Nancy I) for the electron probe microanalyses and the scanning electron microscopy, and to Laboratoire de Physique et Mécanique des Matériaux (Université Paul Verlaine – Metz) for the roughness measurements by interferometric microscopy.

References

1. T. Ohta, T. Kajikawa and Y. Kumashiro, *Electr. Eng. Jpn.* **110** (1990) 213.
2. J.H. Kiely and D.H. Lee, *Meas. Sci. Technol.* **8** (1997) 661.
3. S. Hava, H.B. Sequiera and R.G. Hunsperger, *J. Appl. Phys.* **58** (1985) 1727.
4. D.Y. Lou, *Appl. Opt.* **21** (1982) 1602.
5. A. Ioffe, *Semiconductors Thermoelements and Thermoelectric Cooling* (Infosearch, London, 1957) 81 pp.
6. B. Yim and F. Rosi, *Solid State Electron.* **15** (1957) 1121.
7. M. Schlesinger and M. Paunovic, *Modern Electroplating*, 4th ed., (Electrochemical Society Series, New York, 2000), pp. 868.
8. M. Takahashi, Y. Katou, K. Nagata and S. Furuta, *Thin Solid Films* **240** (1994) 70.
9. P. Magri, C. Boulanger and J.M. Lecuire, *J. Mater. Chem.* **6** (1996) 773.
10. Y. Miyazaki and T. Kajitani, *J. Cryst. Growth* **229** (2001) 542.
11. J.P. Fleurial, A. Borsheevsky, M.A. Ryan, W.M. Phillips, J.G. Snyder, T. Caillat, E.A. Kolawa, J.A. Herman, P. Mueller and M. Nicolet, *Mater. Res. Soc.* **545** (1999) 493.
12. S. Michel, S. Diliberto, C. Boulanger, N. Stein and J.M. Lecuire, *J. Cryst. Growth* **277** (2005) 274.
13. S. Michel, N. Stein, M. Schneider, C. Boulanger and J.M. Lecuire, *J. Appl. Electrochem.* **33**(1) (2003) 23.
14. D. Del Frari, S. Diliberto, N. Stein, C. Boulanger and J.M. Lecuire, *Thin Solid Films* **483** (2005) 44.
15. G.S. Nolas, J. Sharp and H.J. Goldsmid, *Thermoelectrics: Basics Principles and New Materials Developments* (Springer, Berlin, 2001), pp. 292.
16. R.K. Sharma, G. Singh and A.C. Rastogi, *Solar Energy Mat. Solar Cells* **82** (2004) 201.
17. D. Landolt and A. Marlot, *Surf. Coat. Tech.* **169** (2003) 8.
18. S.O. Pagotto, C. Freire and M. Ballester, *Surf. Coat. Tech.* **122** (1999) 10.
19. M. Ghaemi and L. Binder, *J. Power Sources* **111** (2002) 248.
20. N.S. Qu, D. Zhu, K.C. Chan and W.N. Lei, *Surf. Coat. Tech.* **168** (2003) 123.
21. D. Del Frari, S. Diliberto, N. Stein, C. Boulanger and J.M. Lecuire, Electroplating and characterization of $(\text{Bi}_{1-x}\text{Sb}_x)_2\text{Te}_3$ thermoelectric films, proceedings of the 8 European Workshop on Thermoelectrics, Krakow, Poland, 15–17 September (2004).
22. A. Foucaran, A. Sackda, A. Giani, F. Pascal-Delannoy and A. Boyer, *Mater. Sci. Eng.* **B52** (1998) 154.
23. B. Aboulfarah, A. Giani, A. Boyer and A. Mzerd, *Ann. Chim. Sci. Mater.* **25** (2000) 263.